Malaysian Journal of Mathematical Sciences 20(3): 1137–1164 (2026)
https://doi.org/10.47836/mjms.20.3.13

Malaysian Journal of Mathematical Sciences

Journal homepage: https://mjms.upm.edu.my

Block Backward Differentiation Formula with a Singly Diagonally Implicit Structure for Numerical Simulation of Dynamics Models of Diabetes Mellitus

Sunwandi, N. S.[1], Aksah, S. J.[2,3], Rasid, N. A.[2,4], and Ijam, H. M.*[1,2]

[1]*Faculty of Computer and Mathematical Sciences, Universiti Teknologi MARA, 40450 Shah Alam, Selangor, Malaysia*
[2]*Applied Numerical Analysis Research Initiative Group, Faculty of Computer and Mathematical Sciences, Universiti Teknologi MARA, 40450 Shah Alam, Selangor, Malaysia*
[3]*Centre of Foundation Studies, Universiti Teknologi MARA, Cawangan Selangor, Kampus Dengkil, 43800 Dengkil, Selangor, Malaysia*
[4]*Faculty of Computer and Mathematical Sciences, Universiti Teknologi MARA, Perak Branch, Tapah Campus, 35400 Tapah Road, Perak, Malaysia*

E-mail: hazizahijam@uitm.edu.my
**Corresponding author*

Received: 3 September 2025
Accepted: 10 March 2026

Abstract

This paper presents a Singly Diagonally Implicit Block Backward Differentiation Formula of order two for the numerical solution of stiff ordinary differential equations arising in diabetes mellitus models. The proposed method is formulated as a two–step block scheme that computes approximations at two consecutive time levels simultaneously. Its singly diagonally implicit coefficient structure enables sequential solution of the block equations, significantly reducing computational cost per time step while preserving strong stability properties for stiff systems. The performance of the proposed method is investigated using several diabetes models, including models with available analytical solutions. Numerical experiments demonstrate improved accuracy compared with the conventional block backward differentiation formula method and stable, non-oscillatory behavior across a range of stiff parameter regimes. A stability analysis based on the linear test equation confirms that the proposed method is both A–stable and L–stable, ensuring effective damping of rapidly decaying components. These results show that the proposed method is suitable for the efficient and stable numerical simulation of stiff diabetes models.

Keywords: block backward differentiation formula; dynamics models of diabetes mellitus; singly diagonally implicit.

1 Introduction

Recent advances in numerical analysis have highlighted the importance of stability–preserving and efficient numerical schemes for solving nonlinear biological models governed by differential equations. Arif et al. [6] and Ejaz et al. [12] investigated the stability of predator–prey systems with disease dynamics, demonstrating that such models exhibit multiscale behaviour. Arif et al. [7] extended this work to fractional–order systems and showed that stiffness arises due to memory effects and varying time scales. In addition, Arif et al. [8] explored neural network–based approaches for analyzing multi–species systems, further emphasizing the need for robust numerical solvers for complex biological dynamics. Collectively, these works motivate the development of stable and efficient numerical solvers for stiff biological models, including those arising in diabetes dynamics.

Mathematical modelling has become an indispensable tool in the study and management of diabetes mellitus, providing a framework for understanding the intricate dynamics of glucose–insulin regulation [15]. These models often take the form of initial value problems (IVPs), where the goal is to find the solution to ordinary differential equations (ODEs) given specific initial conditions [4]. As noted by Butcher in [10], IVPs are used extensively in science and engineering to model real–world situations such as population growth, motion and the spread of diseases like influenza, malaria and dengue fever.

The increasing prevalence of diabetes mellitus underscores the urgent need for accurate and efficient computational methods to simulate these models. Traditional models of insulin–glucose dynamics have been rooted in physiological principles [24]. However, clinical data is often sparse, which constrains the complexity of the models. The exploration of chaotic behaviour in metabolic systems, particularly in the context of diabetes, is crucial for a deeper understanding of the disease, interactions between glucose and insulin, and possible cures [15]. The genesis of diabetes mellitus is multifaceted, involving various factors that contribute to abnormalities in insulin secretion and function. A mathematical model incorporating time delay has been proposed to describe all glucose–insulin interactions. Such models serve as valuable tools for researchers and clinicians, enabling them to explore different aspects of the disease, test hypotheses and develop strategies for intervention and prevention [5].

The application of numerical methods to these models allows for the simulation of diabetes progression and the evaluation of different treatment strategies [5]. The development of automated insulin–delivery systems relies heavily on mathematical modelling to enhance glycemic control [30]. These models often manifest as systems of ODEs that capture the dynamic interplay between glucose and insulin levels [29]. Models are simplified representations of physiological systems, with the ideal model balancing realism, interpretability and practical application [23]. These models can range from simple linear representations to complex nonlinear systems, each with its own strengths and limitations [25]. It has been shown that such models can determine the nature of a disease and whether it will spread or be eradicated [13].

The simulation of diabetes models often requires the use of numerical methods to approximate the solutions of these differential equations [11]. The accuracy and efficiency of these numerical methods are crucial for obtaining reliable results and making informed decisions. Implicit numerical methods have been widely used to address stiffness in ODE systems. Lambert [21] defined stiffness in terms of eigenvalue distributions, highlighting the need for methods that remain stable for large step sizes. Among these, the backward differentiation formula (BDF) has proven particularly effective for stiff systems. However, classical BDF methods require solving fully coupled nonlinear systems, leading to high computational cost.

To improve efficiency, block backward differentiation formula (BBDF) methods have been developed to compute multiple solution points simultaneously. Akinfenwa et al. [1] introduced continuous BBDF methods to enhance accuracy for stiff ODEs. Ibrahim et al. [17] analyzed the efficiency of block methods and demonstrated their advantages over existing BBDF methods of the same order. Noor et al. [26] further extended the framework in [18] and [31] by developing a fractional BBDF that improves stability and accuracy for stiff systems. Subsequent work [28] proposed an optimized block method based on collocation and interpolation techniques and demonstrated its applicability to highly stiff systems. These studies collectively show that block methods can significantly reduce computational effort while maintaining stability.

Recent advancements in mathematical modelling have uncovered a growing number of systems exhibiting stiffness, a phenomenon that challenges the effectiveness of traditional numerical methods [19]. Stiffness occurs in a system when there are widely varying time scales, necessitating extremely small time steps to ensure both stability and accuracy. Stiffness is most commonly characterized using the eigenvalues of the Jacobian matrix. As defined in [21], an IVP for a first–order ODE is considered stiff if the eigenvalues, λ_i of $\dfrac{\partial f}{\partial y}$ satisfy the conditions $Re(\lambda_i) < 0$ and $\max\limits_i |Re(\lambda_i)| \gg \min\limits_i |Re(\lambda_i)|$, resulting in a stiffness ratio $\dfrac{\max\limits_i |Re(\lambda_i)|}{\min\limits_i |Re(\lambda_i)|} > 1$. The concept of $A-$stability was introduced to address the challenges posed by stiffness in the numerical solution of IVPs. For stiff ODEs, it is essential to design accurate algorithms with strong stability properties, as stability is known to be a significant limitation of block methods [17].

One approach to improving the efficiency of implicit methods, particularly with respect to reducing computational cost and simplifying implementation, is to introduce a diagonally implicit structure. In this structure, the coefficient matrix is arranged in a form that allows for easier inversion. Diagonally Implicit Runge–Kutta (DIRK) methods are a class of implicit methods that exhibit this property, offering a practical balance between numerical stability and computational efficiency [20][22]. A singly diagonally implicit BBDF further enhances this approach by reducing a fully implicit system to a lower triangular matrix with identical diagonal elements. This configuration requires only one evaluation of the Jacobian and a single lower-upper (LU) decomposition per time step [3], thereby significantly lowering the computational burden. Consequently, the method achieves greater efficiency, particularly when applied to stiff systems where such operations are typically computationally intensive.

The development of BBDF methods with a singly diagonally implicit structure presents a promising approach for the accurate and efficient simulation of diabetes models. The singly diagonally implicit structure enables more efficient implementation in terms of reduced computational cost and lower memory requirements, as it requires fewer Jacobian evaluations and matrix factorizations per time step. Meanwhile, the block formulation contributes to improved stability and accuracy, particularly when dealing with systems exhibiting stiff dynamics. The advantages of implicit methods for stiff systems are well documented in [20] and [32], as these methods allow for larger time steps without sacrificing stability and are capable of handling rapid changes in certain components of the solution, which are common in stiff systems. This makes them especially suitable for simulating complex biological processes, such as glucose–insulin dynamics in diabetes models.

Despite the advancements in BBDF and its variants, the construction of singly diagonally implicit structured BBDF methods remains relatively limited. Many existing BBDF implementations still rely on fully implicit formulations, which incur higher computational costs due to the need for Jacobian evaluations and LU decompositions at each step [19]. The integration of singly diago-

nally implicit structures within BBDF frameworks represents a promising direction for enhancing numerical efficiency by reducing computational complexity [3], while preserving the favourable stability properties inherent in BDF methods. Therefore, this paper explores the development and application of a BBDF method with a singly diagonally implicit structure for simulating the dynamics of diabetes mellitus models, which predicts the risk level classification of diabetic patient.

In this study, three well–established mathematical models of diabetes are employed as benchmark test problems to evaluate the performance of the proposed numerical method. The first model is a diabetes complication (DC) model introduced by Boutayeb et al. in [9], which describes the long–term progression of diabetes–related complications through a system of nonlinear ODEs. The second model is an extended DC model analyzed by AlShurbaji et al. in [5], which incorporates additional interaction terms and parameters, resulting in increased stiffness and numerical complexity. The third model is a lifestyle–intervention–based Type 2 Diabetes model developed by Ferdous in [13], which captures the impact of behavioural and treatment interventions on glucose–insulin dynamics. From a modelling perspective, this metabolic–based formulation is conceptually related to the classical Bergman Minimal Model, which is widely used to describe glucose–insulin dynamics and assess the metabolic state of diabetic systems.

These models are well documented in the literature and are known to exhibit stiff behaviour arising from inherent multiscale dynamics, where fast metabolic processes such as glucose–insulin interactions coexist with slow physiological mechanisms including disease progression and complication development. This separation of time scales leads to stiffness under certain parameter regimes, making the models both suitable and challenging test problems. Consequently, they provide a meaningful benchmark for evaluating the stability, accuracy and computational efficiency of stiff numerical solvers, including the proposed singly diagonally implicit BBDF method.

Mathematical models of diabetes are increasingly used to investigate metabolic dynamics and long–term complication development. These models typically exhibit strong stiffness and multiscale behavior due to the coexistence of fast metabolic processes and slow pathological progression. As a result, the accuracy, stability and efficiency of the underlying numerical solvers play a crucial role in the reliability of simulation outcomes. The main motivation of this study is therefore to develop and assess a robust singly diagonally implicit BBDF capable of efficiently solving stiff diabetes models and providing reliable numerical approximations that can support future simulation–based investigations in computational health sciences.

2 Derivation of the Method

In this section, the derivation of $\rho-$Singly Diagonally Implicit Block Backward Differentiation Formula of order 2 ($\rho-$SDIBBDF(2)) will be presented in detail. $\rho-$SDIBBDF(2) is an extended version of BBDF formulated by Ijam and Ibrahim [19] and Aksah et al. [3]. Figure 1 shows the mechanism of the proposed method.

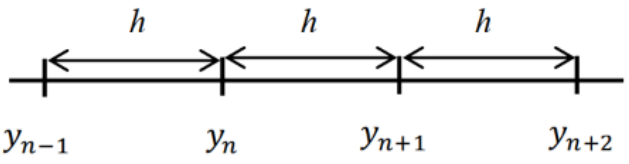

Figure 1: $2-$point $\rho-$SDIBBDF(2) method of fixed step size, h

The most efficient ODE solvers have evolved over the years through advancements in conventional Runge–Kutta (RK) methods. Ibrahim et al. [18] analyzed the efficiency of these methods by comparing them with both a fully implicit multistep method (BBDF) and explicit one-step methods (such as RK and Euler's method). By incorporating singly diagonally implicit properties, the enhanced RK approaches demonstrated superior computational performance compared to existing methods. A method with equal diagonal elements, denoted by $a_{ii} = \gamma$, classified as a Singly Diagonally Implicit Runge–Kutta (SDIRK) method, one of the early formulations of which is depicted in the Butcher tableau of Figure 2, as originally presented in [27].

c_1	γ	0	$\cdots$	0
c_2	a_{21}	γ	$\cdots$	0
$\vdots$	$\vdots$	$\vdots$		$\vdots$
c_n	a_{n1}	a_{n2}	$\cdots$	γ
	b_1	b_2	$\cdots$	b_n

Figure 2: Butcher array of DIRK in [27]

The choice of a singly diagonally implicit structure is motivated by computational efficiency considerations. In fully implicit block methods, all stage equations are coupled and must be solved simultaneously, leading to large nonlinear systems and increased computational cost per Newton iteration. In contrast, the singly diagonally implicit formulation requires solving only one implicit equation per block stage, which significantly reduces the number of Jacobian evaluations and matrix factorizations. This structure preserves the ability to handle stiffness effectively while offering substantial computational savings, making it particularly suitable for long-term simulations of stiff dynamical systems such as diabetes models.

The $\rho-$SDIBBDF(2) method is derived through the Lagrange series polynomial interpolation method. The general formula of the proposed method is in the form of

$$\sum_{i=0}^{w} \alpha_{k,i-1} y_{n+i-1} = h\beta_{k,w}(f_{n+k} - \rho f_{n+k-1}), \tag{1}$$

where $w = k+m-1$. From Equation (1), the linear difference operator, $\mathcal{L}$, for the block multistep method is defined as

$$\mathcal{L}_k[y(x_n); h] = \sum_{i=0}^{w} \alpha_{k,i-1} y(x + (i-1)h) - h\beta_{k,w}[y'(x+kh) - \rho y'(x+(k-1)h)], \tag{2}$$

where $m = 2$ is the order of the methods and $k = 1, 2$ for solutions points y_{n+1} and y_{n+2}, respectively. Formulation of $\rho-$SDIBBDF(2) consist of interpolating of y at points (x_{n-1}, y_{n-1}), (x_n, y_n), (x_{n+1}, y_{n+1}) and (x_{n+2}, y_{n+2}).

For y_{n+1}, the expansion of polynomial in Equation (2) can be written as follows

$$\begin{aligned} P(x) = &\frac{(x-x_n)(x-x_{n+1})}{(x_{n-1}-x_n)(x_{n-1}-x_{n+1})} y_{n-1} + \frac{(x-x_{n-1})(x-x_{n+1})}{(x_n-x_{n-1})(x_n-x_{n+1})} y_n \\ &+ \frac{(x-x_{n-1})(x-x_n)}{(x_{n+1}-x_{n-1})(x_{n+1}-x_n)} y_{n+1}. \end{aligned} \tag{3}$$

By assigning $x = x_{n+1} + sh$ and substitute into Equation (3) yields

$$\begin{aligned} P(x) = &\frac{(sh - x_n + x_{n+1})sh}{(x_{n-1} - x_n)(x_{n-1} - x_{n+1})} y_{n-1} + \frac{(sh - x_{n-1} + x_{n+1})sh}{(x_n - x_{n-1})(x_n - x_{n+1})} y_n \\ &+ \frac{(sh - x_{n-1} + x_{n+1})(sh - x_n + x_{n+1})}{(x_{n+1} - x_{n-1})(x_{n+1} - x_n)} y_{n+1}. \end{aligned} \tag{4}$$

Then, by substituting the difference between each point and the preceding value x_{n-1} and letting $x_{n-1} = 0, x_n = h$ and $x_{n+1} = 2h$ into Equation (4), we obtain

$$P(x) = \frac{1}{2}\frac{(sh + h)s}{h} y_{n-1} - \frac{(sh + 2h)s}{h} y_n + \frac{1}{2}\frac{(sh + 2h)(sh + h)}{h^2} y_{n+1}. \tag{5}$$

Next, differentiating Equation (5) with respect to s yields the following equation

$$P'(x) = \frac{1}{2} s y_{n-1} + \frac{1}{2}\frac{(sh + h)}{h} y_{n-1} - s y_n - \frac{(sh + 2h)}{h} y_n + \frac{1}{2}\frac{(sh + h)}{h} y_{n+1} + \frac{1}{2}\frac{(sh + 2h)}{h} y_{n+1}. \tag{6}$$

By considering $hf_{n+1} = P'(x_{n+1})$, we set $x = x_n$ to determine the value of s to be substituted into Equation (6), where

$$\begin{aligned} x_{n+1} + sh &= x_n, \\ sh &= x_n - x_{n+1}, \\ sh &= -h, \\ s &= -1. \end{aligned}$$

Upon substituting $s = -1$ into Equation (6), the resulting expression is obtain as

$$hf_n = -\frac{1}{2} y_{n-1} + \frac{1}{2} y_{n+1}. \tag{7}$$

Subsequently, setting $x = x_{n+1}$, results in $s = 0$, which is then substituted into Equation (6), yielding

$$hf_{n+1} = \frac{1}{2} y_{n-1} - 2y_n + \frac{3}{2} y_{n+1}. \tag{8}$$

By solving $hf_{n+1} - \rho hf_n$ from Equations (7) and (8) for y_{n+1}, we obtain

$$y_{n+1} = \frac{\rho + 1}{\rho - 3} y_{n-1} - \frac{4}{\rho - 3} y_n + \frac{2\rho}{\rho - 3} hf_n - \frac{2}{\rho - 3} hf_{n+1}. \tag{9}$$

To determine y_{n+2}, Equation (2) is expanded, leading to the following equation

$$\begin{aligned} P(x) = &\frac{(x - x_{n+1})(x - x_{n+2})}{(x_n - x_{n+1})(x_n - x_{n+2})} y_n + \frac{(x - x_n)(x - x_{n+2})}{(x_{n+1} - x_n)(x_{n+1} - x_{n+2})} y_{n+1} \\ &+ \frac{(x - x_n)(x - x_{n+1})}{(x_{n+2} - x_n)(x_{n+2} - x_{n+1})} y_{n+2}. \end{aligned} \tag{10}$$

Similarly, defining $x = x_{n+2} + sh$ and substituting into Equation (10) yields the following result

$$\begin{aligned} P(x) = &\frac{(sh - x_{n+1} + x_{n+2})sh}{(x_n - x_{n+1})(x_n - x_{n+2})} y_n + \frac{(sh - x_n + x_{n+2})sh}{(x_{n+1} - x_n)(x_{n+1} - x_{n+2})} y_{n+1} \\ &+ \frac{(sh - x_n + x_{n+2})(sh - x_{n+1} + x_{n+2})}{(x_{n+2} - x_n)(x_{n+2} - x_{n+1})} y_{n+2}. \end{aligned} \tag{11}$$

Then, by replacing the difference between each point and the previous value x_{n-1} and substituting $x_{n-1} = 0, x_n = h, x_{n+1} = 2h$ and $x_{n+2} = 3h$ into Equation (11), the result is

$$P(x) = \frac{1}{2}\frac{(sh+h)s}{h}y_n - \frac{(sh+2h)s}{h}y_{n+1} + \frac{1}{2}\frac{(sh+2h)(sh+h)}{h^2}y_{n+2}. \tag{12}$$

Next, differentiate Equation (12) with respect to s yields the following result

$$P'(x) = \frac{1}{2}sy_n + \frac{1}{2}\frac{(sh+h)}{h}y_n - sy_{n+1} - \frac{(sh+2h)}{h}y_{n+1} + \frac{1}{2}\frac{(sh+h)}{h}y_{n+2} + \frac{1}{2}\frac{(sh+2h)}{h}y_{n+2}. \tag{13}$$

Considering $hf_{n+2} = P'(x_{n+2})$, $x = x_{n+1}$ is set to determine the value of s, which is then substituted into Equation (13), where

$$\begin{aligned} x_{n+2} + sh &= x_{n+1}, \\ sh &= x_{n+1} - x_{n+2}, \\ sh &= -h, \\ s &= -1. \end{aligned}$$

Then, by substituting $s = -1$ into Equation (13), the following result is obtain

$$hf_{n+1} = -\frac{1}{2}y_n + \frac{1}{2}y_{n+2}. \tag{14}$$

Next, setting $x = x_{n+2}$ results in $s = 0$, which is then substituted into Equation (13), yielding

$$hf_{n+2} = \frac{1}{2}y_n - 2y_{n+1} + \frac{3}{2}y_{n+2}. \tag{15}$$

Upon solving $hf_{n+2} - \rho hf_{n+1}$ from Equations (14) and (15) for y_{n+2}, gives

$$y_{n+2} = \frac{\rho+1}{\rho-3}y_n - \frac{4}{\rho-3}y_{n+1} + \frac{2\rho}{\rho-3}hf_{n+1} - \frac{2}{\rho-3}hf_{n+2}. \tag{16}$$

As suggested by Ijam and Ibrahim [19], the free parameter ρ is selected within the interval $(-1, 1)$ to ensure absolute stability. In this study, $\rho = -0.75$ is adopted to achieve accurate numerical results with optimal stability properties, making the method well–suitable for solving stiff problems. A detailed justification for this selection of ρ is provided in [19]. By substituting $\rho = -0.75$ into Equations (9) and (16), the proposed method can be expressed in matrix form as follows,

$$\begin{bmatrix} \frac{1}{15} & -\frac{16}{15} \\ 0 & \frac{1}{15} \end{bmatrix}\begin{bmatrix} y_{n-1} \\ y_n \end{bmatrix} + \begin{bmatrix} 1 & 0 \\ -\frac{16}{15} & 1 \end{bmatrix}\begin{bmatrix} y_{n+1} \\ y_{n+2} \end{bmatrix} = h\begin{bmatrix} 0 & \frac{2}{5} \\ 0 & 0 \end{bmatrix}\begin{bmatrix} f_{n-1} \\ f_n \end{bmatrix} + h\begin{bmatrix} \frac{8}{15} & 0 \\ \frac{2}{5} & \frac{8}{15} \end{bmatrix}\begin{bmatrix} f_{n+1} \\ f_{n+2} \end{bmatrix} \tag{17}$$

with

$$A_0 = \begin{bmatrix} \frac{1}{15} \\ 0 \end{bmatrix}, A_1 = \begin{bmatrix} -\frac{16}{15} \\ \frac{1}{15} \end{bmatrix}, A_2 = \begin{bmatrix} 1 \\ -\frac{16}{15} \end{bmatrix}, A_3 = \begin{bmatrix} 0 \\ 1 \end{bmatrix}, B_0 = \begin{bmatrix} 0 \\ 0 \end{bmatrix}, B_1 = \begin{bmatrix} \frac{2}{5} \\ 0 \end{bmatrix}, B_2 = \begin{bmatrix} \frac{8}{15} \\ \frac{2}{5} \end{bmatrix}, B_3 = \begin{bmatrix} 0 \\ \frac{8}{15} \end{bmatrix}.$$

In accordance with standard linear multistep method (LMM) terminology, the proposed $\rho-$SDIBBDF(2) method is implemented using a PECE sequence, where P and C denote the predictor and corrector stages, respectively and E represents function evaluation. The computational procedure is summarized as follows.

Step 1: Predictor (P)
For each block and stage j, initial approximations $y_{n+j}^{(p)}$, are obtained using the explicit predictor formula based on previously computed solution values.

$$y_{n+1}^{(p)} = -y_{n-1} + 2y_n, \quad y_{n+2}^{(p)} = -2y_{n-1} + 3y_n.$$

Step 2: Evaluation (E)
The right-hand side function is evaluated at the predicted values,

$$f(x_{n+j}, y_{n+j}^{(p)}).$$

Step 3: Corrector (C)
A more accurate approximation $y_{n+j}^{(c)}$ is computed using the implicit corrector formula. Owing to the singly diagonally implicit structure, the block stage equations are solved sequentially, with each stage depending only on previously computed stages.

Step 4: Evaluation (E)
The function is re-evaluated at the corrected values,

$$f(x_{n+j}, y_{n+j}^{(c)}),$$

to complete the PECE cycle for the current block.

The solution is then advanced to the next block, and the procedure is repeated until the final integration time is reached. This sequential PECE–based implementation significantly reduces computational complexity compared to fully implicit block schemes while preserving stability for stiff problems.

3 Stability Analysis of The Method

This section focuses on the order, convergence and stability of the proposed method. The following definitions clarify the concepts of zero stability, $A-$stability, consistency and explain how they relate to the notion of convergence.

Zero stability is a fundamental requirement for the convergence of LMM. It ensures that the numerical solution remains bounded in response to small perturbations in the initial data as the step size tends to zero, which is crucial to prevent the amplification of errors and to guarantee that the numerical solution closely follows the behaviour of the exact solution.

Definition 3.1. *The LMM is said to have zero stability if no root of its characteristic polynomial has a modulus higher than one and if any root with a modulus of one is simple* [21].

Consider the scalar test equation $y' = \lambda y$. By substituting $h\lambda = H$ into Equations (9) and (16) and rewriting it in matrix form, we obtain

$$\underbrace{\begin{bmatrix} 1 + \frac{2}{\rho-3}H & 0 \\ \frac{4}{\rho-3} - \frac{2\rho}{\rho-3}H & 1 + \frac{2}{\rho-3}H \end{bmatrix}}_{P} \begin{bmatrix} y_{n+1} \\ y_{n+2} \end{bmatrix} = \underbrace{\begin{bmatrix} \frac{\rho+1}{\rho-3} & -\frac{4}{\rho-3} + \frac{2\rho}{\rho-3}H \\ 0 & \frac{\rho+1}{\rho-3} \end{bmatrix}}_{Q} \begin{bmatrix} y_{n-1} \\ y_n \end{bmatrix}, \tag{18}$$

which is equivalent to $PY_m = QY_{m-1}$. By substituting the coefficients P and Q from Equation (18) into the determinant expression $|Pr - Q| = 0$, the following stability polynomial is obtain

$$\begin{aligned} SP(r,H) = &-\frac{1}{(\rho-3)^2}(4H^2\rho^2 r - 4H^2 r^2 - 4H\rho r^2 - \rho^2 r^2 - 12H\rho r + 12Hr^2 + 2\rho^2 r \\ &+ 6\rho r^2 + 4Hr - \rho^2 - 4\rho r - 9r^2 - 2\rho + 10r - 1). \end{aligned} \tag{19}$$

By evaluating $SP(r,0)$ for $\rho = -0.75$, the resulting roots are

$$r_1 = 1, r_2 = \frac{1}{225}.$$

Zero stability of the $\rho-$SDIBBDF(2) method is confirmed when the roots of $SP(r,H)$, as given in Equation (19), meet the requirements of Definition 3.1.

The regions of absolute stability are presented to illustrate the stability characteristics of the proposed methods. As noted by [14], a larger stability region permits the use of larger step sizes while maintaining control over truncation error, which is particularly beneficial for stiff systems.

Definition 3.2. *A numerical method is said to be $A-$stable if $\Re_A \supseteq \{H \mid \mathrm{Re}(H) < 0\}$. This means that the stability region covers the whole left-hand of the H-plane as shown in Figure 3.*

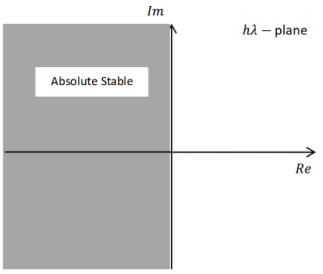

Figure 3: Absolute stability region of an $A-$stable method

The stability region is obtained by substituting $r = e^{i\theta}$ into Equation (19) and solving $SP(r,H)$ for r. The resulting stability boundary, corresponding to values of $\theta \in [0, 2\pi]$ for which $|r| < 1$, is plotted using MAPLE software and illustrated in Figure 4.

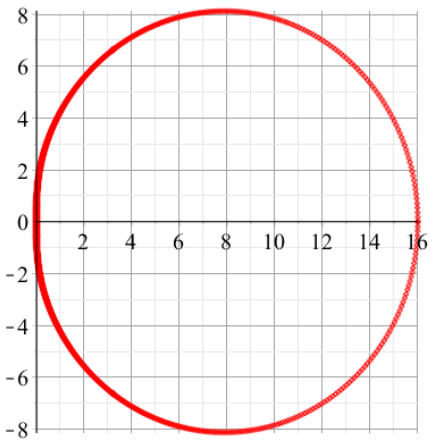

Figure 4: Stability region for $\rho-$SDIBBDF(2) for $\rho = -0.75$

As shown in Figure 4, the region of absolute stability lies outside the closed contour of the graph, while the unstable region is contained within it. In accordance with Definition 3.2, it is concluded that the $\rho-$SDIBBDF(2) method possesses $A-$stable properties.

Definition 3.3. *A numerical method is said to be $L-$stable if it is $A-$stable and its stability function $R(H)$ satisfies $\lim_{H\to\infty} R(H) = 0$.*

The $L-$stability of the proposed method is examined using the standard linear test equation $y' = \lambda y$, where $\mathrm{Re}(\lambda) < 0$. Applying the proposed scheme to this equation yields the stability function $R(H)$, with $H = h\lambda$. The method is $A-$stable, as the resulting stability region covers the entire left–hand of the $H-$plane. Furthermore, taking the limit of the stability function as $H \to \infty$ gives $\lim_{H\to\infty} R(H) = 0$, which confirms that the proposed method strongly damps stiff components. Therefore, the proposed method is $L-$stable and well suited for stiff systems such as diabetes models. This property ensures strong damping of rapidly decaying components and explains the method's ability to handle highly stiff diabetes models efficiently, even for moderate step sizes. The observed numerical robustness contrasts with adaptive solvers such as ode15s, which require substantially tighter tolerances to achieve comparable stability in stiff regimes.

Convergence is a fundamental property that reflects the effectiveness of a numerical method. It ensures that the approximate solution approaches the exact solution of the differential equation as the step size tends to zero. Typically, convergence requires that the method be both consistent and zero-stable [16]. According to Lambert [21], the consistency conditions outlined in Definition 3.3 must be satisfied for the convergence theorem to hold.

Definition 3.4. *The LMM is said to be consistent if it has order $p \geq 1$. The method is consistent if and only if the following conditions are satisfied:*

$$a)\ \sum_{j=0}^{3} A_j = 0,$$

$$b)\ \sum_{j=0}^{3} jA_j = \sum_{j=0}^{3} B_j.$$

By applying the above consistency conditions to the respective coefficients of y_{n+1} and y_{n+2} in Equation (17), we obtain:

$$\text{a)}\ \sum_{j=0}^{3} A_j = \begin{bmatrix} \frac{1}{15} \\ 0 \end{bmatrix} + \begin{bmatrix} -\frac{16}{15} \\ \frac{1}{15} \end{bmatrix} + \begin{bmatrix} 1 \\ -\frac{16}{15} \end{bmatrix} + \begin{bmatrix} 0 \\ 1 \end{bmatrix} = \begin{bmatrix} 0 \\ 0 \end{bmatrix},$$

$$\text{b)}\ \sum_{j=0}^{3} jA_j = 0\begin{bmatrix} \frac{1}{15} \\ 0 \end{bmatrix} + 1\begin{bmatrix} -\frac{16}{15} \\ \frac{1}{15} \end{bmatrix} + 2\begin{bmatrix} 1 \\ -\frac{16}{15} \end{bmatrix} + 3\begin{bmatrix} 0 \\ 1 \end{bmatrix} = \begin{bmatrix} \frac{14}{15} \\ \frac{14}{15} \end{bmatrix},$$

$$\sum_{j=0}^{3} B_j = \begin{bmatrix} 0 \\ 0 \end{bmatrix} + \begin{bmatrix} \frac{2}{5} \\ 0 \end{bmatrix} + \begin{bmatrix} \frac{8}{15} \\ \frac{2}{5} \end{bmatrix} + \begin{bmatrix} 0 \\ \frac{8}{15} \end{bmatrix} = \begin{bmatrix} \frac{14}{15} \\ \frac{14}{15} \end{bmatrix}.$$

According to Definition 3.4, the consistency of $\rho-$SDIBBDF(2) is assured, as the method has an order $p \geq 1$. Hence, the proposed method is proven to be convergent, since it is consistent and zero stable.

4 Mathematical Model

The numerical experiments are conducted using three diabetes–related dynamical models taken from the literature. The DC model by Boutayeb et al. [9] and the extended DC model by AlShurbaji et al. [5] are employed to examine the behaviour of the proposed method under stiff conditions arising from multiscale disease dynamics. In addition, a lifestyle–intervention–based Type 2 Diabetes model proposed by Ferdous [13] is used to evaluate the method's capability in capturing long–term intervention effects. These models collectively provide a diverse and representative set of stiff test problems for assessing numerical accuracy, stability and computational efficiency.

This section also addresses the dynamics of diabetes mellitus using systems of ODEs modelled in [5], [9] and [13], which integrate key factors such as disease progression, complications and the influence of lifestyle changes. The equations describe interactions among populations affected by diabetes, including those with and without complications and incorporate variables such as treatment rates, mortality and preventive measures. Parameters are selected to reflect real–world scenarios, offering insight into the incidence of diabetes, its associated complications and the benefits of healthy lifestyle interventions. By combining these elements, the system provides a comprehensive framework for predicting outcomes and evaluating strategies for disease management and prevention.

4.1 Model A

Boutayeb et al. [9] presented a foundational model using ODEs, also known as the DC model. It is divided into two categories, diabetics with complications (C) and diabetics without complications (D), incorporating parameters such as the natural mortality rate (μ), the probability of developing complications (λ) and the rate at which complications are cured (γ). A mathematical model has been presented to cope with the dynamics of a diabetic population as follows

$$C'(t) = -(\lambda + \theta)C(t) + \lambda N(t),$$
$$N'(t) = I(t) - (\nu + \delta)C(t) - \mu N(t).$$

where $C(t)$ is the number of diabetics with complication and let $N(t) = C(t)+D(t)$ denote the size of population of diabetics at time t, with eigenvalues $-0.7722, -0.1077$ and stiffness ratio 7.1699. The initial conditions are

$$C_0 = 47,000,500, \quad N_0 = 61,100,500, \quad 0 \leq t \leq 4$$

and the analytical solutions for Model A are provided as follows

$$C(t) = K_1 e^{-\eta_1 t} + K_2 e^{-\eta_2 t} + \frac{\alpha}{\beta} I(t),$$

$$N(t) = K_1 e^{-\eta_1 t} + K_2 e^{-\eta_2 t} + \frac{\alpha}{\beta} I(t) + \frac{\theta}{\lambda} K_1 e^{-\eta_1 t} + \frac{\theta}{\lambda} K_2 e^{-\eta_2 t} + \frac{\theta\alpha}{\lambda\beta} I(t) - \frac{1}{\lambda}(\eta_1 K_1 e^{-\eta_1 t} + \eta_2 K_2 e^{-\eta_2 t}),$$

where the parameters are defined as

$$\begin{aligned}
\theta &= \gamma + \mu + \nu + \delta, \\
\eta_1 &= \frac{1}{2}\left(\sigma - \sqrt{\sigma^2 - 4\beta}\right), \\
\eta_2 &= \frac{1}{2}\left(\sigma + \sqrt{\sigma^2 - 4\beta}\right), \\
\sigma &= \lambda + \theta + \mu, \\
\beta &= \lambda(\nu + \delta) + \mu(\lambda + \theta), \\
\alpha &= \lambda, \\
K_1 &= \frac{\beta(\lambda + \theta - \eta_2)C_0 + I(\alpha\eta_2) - \lambda\beta N_0}{\beta(\eta_1 - \eta_2)}, \\
K_2 &= \frac{-\beta(\lambda + \theta - \eta_1)C_0 + I(-\alpha\eta_1) + \lambda\beta N_0}{\beta(\eta_1 - \eta_2)}.
\end{aligned}$$

The parameters and values of the ODEs for Model A are defined in Table 1 as follows.

Table 1: List of parameters and values used for Model A.

Parameter	Description	Value
ν	Rate at which patients with complications become severely disable	0.05
δ	Mortality rate due to complications	0.05
μ	Natural mortality rate	0.02
γ	Rate at which complications are cured	0.08
λ	Probability of developing a complication	0.66
$I(t)$	Incidence of diabetes mellitus	6×10^6

Figure 5 illustrates the DC model developed by [9], which is used to analyze and control the dynamics of diabetes epidemiology over time.

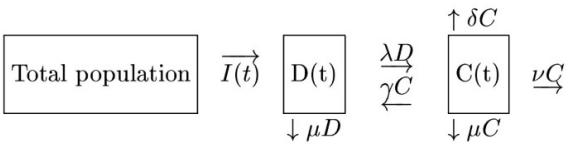

Figure 5: Schematic presentation of Model A by Boutayeb et al. [9]

4.2 Model B

Model B is a mathematical model developed to simulate the population dynamics of diabetes and its associated complications. Originally introduced by Boutayeb et al. [9], it is widely known as the DC model. AlShurbaji et al. [5] extended the analysis of the DC model, as discussed in Akinsola and Oluyo [2], using advanced numerical methods. The model focuses on understanding how diabetes affects population trends over time and how related complications evolve. Several numerical methods are used to analyse the model, including explicit Euler, implicit Euler, Heun's method, the fourth–order Runge–Kutta method and the Adams–Moulton method. These approaches allow for detailed monitoring of the diabetic population and provide valuable insights

into the progression of the disease and its complications over a specified period. The system of ODEs for Model B is represented as follows

$$C'(t) = I(t) - (\lambda + \theta)C(t) + \lambda N(t), \quad t > 0,$$
$$N'(t) = 2I(t) - (\nu + \delta)C(t) - \mu N(t), \quad t > 0.$$

Thus, the analytical solutions for Model B were utilized to determine the true values of $C(t)$ and $N(t)$. These true values served as a basis for comparison and for calculating the percentage error.

$$C(t) = K_1 e^{-\eta_1 t} + K_2 e^{-\eta_2 t} + \frac{\alpha}{\beta} I(t),$$

$$N(t) = K_1 e^{-\eta_1 t} + K_2 e^{-\eta_2 t} + \frac{\alpha}{\beta} I(t) + \frac{\theta}{\lambda} K_1 e^{-\eta_1 t} + \frac{\theta}{\lambda} K_2 e^{-\eta_2 t} + \frac{\theta\alpha}{\lambda\beta} I(t) - \frac{I}{\lambda} - \frac{I}{\lambda}(\eta_1 K_1 e^{-\eta_1 t} + \eta_2 K_2 e^{-\eta_2 t}),$$

where the parameters are defined as

$$\begin{aligned}
\theta &= \gamma + \mu + \nu + \delta, \\
\eta_1 &= \frac{1}{2}\left(\sigma - \sqrt{\sigma^2 - 4\beta}\right), \\
\eta_2 &= \frac{1}{2}\left(\sigma + \sqrt{\sigma^2 - 4\beta}\right), \\
\sigma &= \lambda + \theta + \mu, \\
\beta &= \lambda(\nu + \delta) + \mu(\lambda + \theta), \\
\alpha &= 2\lambda + \mu, \\
K_1 &= \frac{\beta(\lambda + \theta - \eta_2)C_0 + I(\alpha\eta_2 - \beta) - \lambda\beta N_0}{\beta(\eta_1 - \eta_2)}, \\
K_2 &= \frac{-\beta(\lambda + \theta - \eta_1)C_0 + I(\beta - \alpha\eta_1) + \lambda\beta N_0}{\beta(\eta_1 - \eta_2)}.
\end{aligned}$$

The initial conditions are taken from [2] and are given as follows:

$$C^*(t) = \frac{(2\lambda + \mu)I}{\lambda(\nu + \delta + \mu) + \mu\theta}, \qquad N^*(t) = \frac{(2(\lambda + \theta) - (\mu + \delta))I}{\lambda(\nu + \delta + \mu) + \mu\theta},$$

$$C_0 = C^* \pm 500, \qquad N_0 = N^* \pm 500,$$
$$C_0 = 9.021029021 \times 10^7, \qquad N_0 = 1.505249755 \times 10^8, \quad 0 \le t \le 20.$$

The eigenvalues are $-1.4087, -0.0812$ and stiffness ratio is 17.3485. The parameters and values are defined in Table 2 as follows.

Table 2: List of parameters and values used for Model B.

Parameter	Description	Value
λ	Probability of developing a complication	0.85
δ	Mortality rate due to complications	0.05
μ	Natural mortality rate	0.02
γ	Rate at which complications are controlled	0.5
ν	Rate at which patients with complications become severely disable	0.05
$I(t)$	Incidence of diabetes	6×10^6

A schematic presentation of Model B is shown in Figure 6.

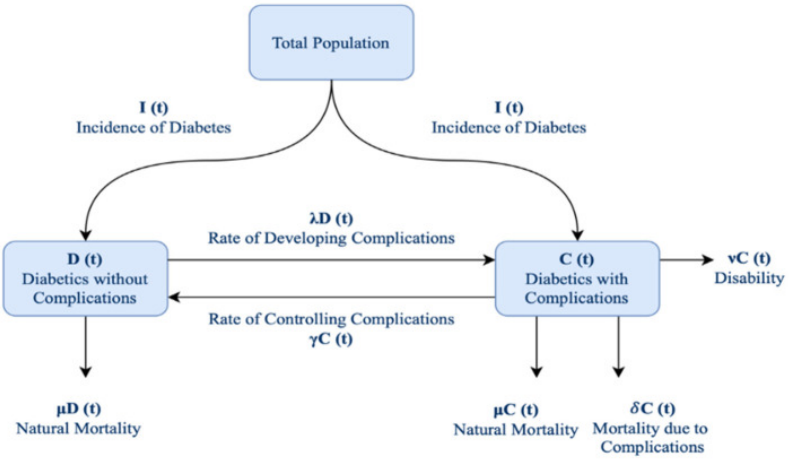

Figure 6: Schematic presentation of Model B by AlShurbaji et al. [5]

4.3 Model C

Ferdous [13] examines the effects of lifestyle interventions on individuals by developing an ODE model. The study constructs a general model based on the dynamics of Type 2 Diabetes (T2D), incorporating a control variable referred to as a healthy lifestyle. The mathematical model of Model C can be represented by the system of ODEs as follows

$$\begin{aligned}
S'(t) &= b - (\mu + \varepsilon + \alpha)S(t),\\
A'(t) &= \varepsilon S(t) - (\tau + \mu + \varepsilon + \delta_1)A(t) + \gamma L(t),\\
T'(t) &= \tau A(t) - (\mu + \delta_2)T(t),\\
L'(t) &= \alpha S(t) - (\gamma + \mu + \beta)L(t),\\
P'(t) &= \beta L(t) - \mu P(t),
\end{aligned}$$

where total adults of age $20-79$ years, $N(t) = S(t)+A(t)+T(t)+L(t)+P(t)$ which is subdivided into five classes which are adults of susceptible class: $S(t)$, adults of affected class: $A(t)$, adults of treated class: $T(t)$, adults maintaining healthy lifestyle: $L(t)$ and adults of prevented class: $P(t)$. The eigenvalues are $-0.0138, -0.0158, -0.3558, -0.3638, -0.6188$ and stiffness ratio is 44.8405. The initial conditions of these variables are considered as

$$S(0) = 1, \quad A(0) = 0, \quad T(0) = 0, \quad L(0) = 0, \quad P(0) = 0, \quad 0 \le t \le 10.$$

Table 3 below represented the list of parameters and values used for the mathematical model.

Table 3: List of parameters and values used for Model C.

Parameter	Description	Value
b	Adult birth rate	$\mu \times 1$
μ	Adult natural mortality rate	0.0138
ε	Rate at which adults become affected from susceptible class	0.142
τ	Treatment rate	0.565
α	Rate at susceptible adults maintaining a healthy lifestyle	0.2
β	Rate at which the healthy lifestyle population goes to the prevented class	0.3
γ	Rate at which adults become affected from healthy lifestyle class	0.05
δ_1	Death rate in class A due to diabetes-related complications	0.04
δ_2	Death rate in class T due to diabetes-related complications	0.002

Figure 7 represents the T2D dynamics model, developed by Ferdous [13], which utilizes a compartmental approach to analyze and control the epidemiological progression of T2D.

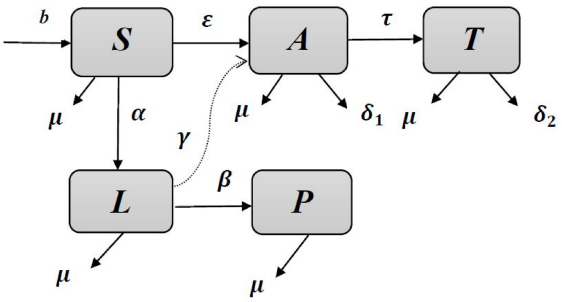

Figure 7: Schematic presentation of Model C by Ferdous [13]

5 Numerical Simulation and Discussion

In this section, the numerical results for Models A, B, and C are presented in Tables 4(a) to 7(e), based on simulations of the proposed mathematical models for diabetes mellitus. Models A, B, and C are solved numerically using the C++ programming language. These numerical results are compared with those obtained using MATLAB's built–in solver, ode15s, which is based on Numerical Differentiation Formulas, a modification of the BDFs.

To validate how good the performance of the model is, the Root of the Mean Squared Error (RMSE) and the Maximum Error (MAXE) are calculated using the numerical solution and the exact solution, respectively

$$\text{RMSE} = \sqrt{\frac{1}{N}\sum_{i=1}^{N}[y(t_i) - y_i]^2}, \quad \text{MAXE} = \max_{1\le i\le TS}\left(\max_{1\le i\le K}|(y_i)_t - (y(t_i))_t|\right),$$

where N is number of observations, TS is the total number of steps, K is the number of equations, y_i and $y(t_i)$ are the approximated and exact solutions, respectively.

Both $\rho-$SDIBBDF(2) and ode15s are being compared with some existing methods in the literature for Model B. The numerical results of the percentage error are given in Tables 6(a) and 6(b),

using

$$\text{Error} = \frac{|y_i - y(t_i)|}{y(t_i)} \times 100\%,$$

where y_i and $y(t_i)$ are the approximated and true values, respectively. The description for abbreviations used in Tables 4(a)–7(e) are provided as follows.

$\rho-$SDIBBDF(2)	$\rho-$Singly Diagonally Implicit Block Backward Differentiation Formula of Order 2
BBDF	Block Backward Differentiation Formula in [18]
ode15s	Variable order solver implemented in numerical differentiation formula in MATLAB
AM(4)	Adam–Moulton (4^{th} order)
RK(4)	Runge–Kutta (4^{th} order)
RMSE	Root Mean Squared Error
MAXE	Maximum error
TIME	Execution time in seconds
TS	Total steps
t	Time in years
I	Increment in t (the time step)

Table 4(a): Approximate solutions of $C(t)$ for Model A

I	Exact Solutions	Approximate Solutions		
		$\rho-$SDIBBDF(2)	BBDF	ode15s
0.00	4.700050000000000E+07	4.70005000000000E+07	4.70005000000000E+07	4.700050000000000E+07
0.01	4.699956560404735E+07	4.69995655979450E+07	4.69995653491052E+07	4.699956601805391E+07
0.02	4.699864433277279E+07	4.69986443266850E+07	4.69986438194006E+07	4.699864598561987E+07
0.05	4.699595822005697E+07	4.69959582140102E+07	4.69959569566818E+07	4.699596830153238E+07
0.10	4.699173407405169E+07	4.69917340680723E+07	4.69917316420601E+07	4.699177267972719E+07
0.20	4.698418793083506E+07	4.69841879249886E+07	4.69841834460388E+07	4.698432936867639E+07
0.50	4.696793651586237E+07	4.69679365103554E+07	4.69679277803283E+07	4.696816978175013E+07
1.00	4.695751743664486E+07	4.69575174315862E+07	4.69575060495712E+07	4.695808939156747E+07
2.00	4.697478328771753E+07	4.69747832832234E+07	4.69747742798144E+07	4.697557646166351E+07
2.50	4.699375352646633E+07	4.69937535220929E+07	4.69937469175541E+07	4.699424468171674E+07
3.00	4.701609036180633E+07	4.70160903575689E+07	4.70160861589810E+07	4.701626771297257E+07
3.50	4.704022018680218E+07	4.70402201826674E+07	4.70402181669478E+07	4.704018750572370E+07
4.00	4.706509942206879E+07	4.70650994179621E+07	4.70650992747506E+07	4.706492576816364E+07
	RMSE	5.02262488547227E-03	5.41019646500097E+00	

Table 4(b): Approximate solutions of $N(t)$ for Model A

I	Exact Solutions	Approximate Solutions		
		$\rho-$SDIBBDF(2)	BBDF	ode15s
0.00	6.11005000000000E+07	6.11005000000000E+07	6.11005000000000E+07	6.11005000000000E+07
0.01	6.11012797911323E+07	6.11012797901961E+07	6.11012797755648E+07	6.11012798148792E+07
0.02	6.11020603532556E+07	6.11020603523209E+07	6.11020603227626E+07	6.11020604488473E+07
0.05	6.11044065386419E+07	6.11044065377113E+07	6.11044064664831E+07	6.11044071072258E+07
0.10	6.11083310701964E+07	6.11083310692724E+07	6.11083309385814E+07	6.11083331344230E+07
0.20	6.11162278862235E+07	6.11162278853129E+07	6.11162276704142E+07	6.11162345581087E+07
0.50	6.11401992357388E+07	6.11401992348564E+07	6.11401989968027E+07	6.11402042196931E+07
1.00	6.11805332380209E+07	6.11805332371727E+07	6.11805334731982E+07	6.11805113193180E+07
2.00	6.12598176815641E+07	6.12598176807264E+07	6.12598196255626E+07	6.12595752832749E+07
2.50	6.12978331169994E+07	6.12978331161131E+07	6.12978359595107E+07	6.12975161965093E+07
3.00	6.13344347073372E+07	6.13344347064689E+07	6.13344383799323E+07	6.13340898063629E+07
3.50	6.13695108849242E+07	6.13695108840710E+07	6.13695152941926E+07	6.13691536750753E+07
4.00	6.14030154205039E+07	6.14030154196009E+07	6.14030204666569E+07	6.14026570929753E+07
	RMSE	8.58522058294979E-04	2.32767525704804E+00	

Table 4(c): Numerical results for Model A

h	Method	TS	MAXE	TIME
10^{-2}	$\rho-$SDIBBDF(2)	200	1.97681E-01	1.83072E-04
	BBDF	200	1.12472E-01	6.12252E-04
10^{-4}	$\rho-$SDIBBDF(2)	20000	5.83197E-03	2.53995E-03
	BBDF	20000	1.14785E-02	8.66723E-03
10^{-6}	$\rho-$SDIBBDF(2)	2000000	6.25596E-05	1.31126E-02
	BBDF	2000000	1.16043E-04	7.15754E-02

Table 5(a): Approximate solutions of $C(t)$ for Model B

t	Exact Solutions	Approximate Solutions		
		$\rho-$SDIBBDF(2)	BBDF	ode15s
0	9.021029021000000E+07	9.02102902100000E+07	9.02102902100000E+07	9.021029021000000E+07
1	9.089269403830102E+07	9.08926940496138E+07	9.08926982613182E+07	9.089010161296606E+07
2	9.100624586293071E+07	9.10062458668285E+07	9.10062498076313E+07	9.100619596409823E+07
3	9.098490242250315E+07	9.09849024242750E+07	9.09849029958577E+07	9.098487489324851E+07
4	9.093441504115434E+07	9.09344150423936E+07	9.09344152309540E+07	9.093435791249400E+07
5	9.088033462020494E+07	9.08803346213668E+07	9.08803343554921E+07	9.088045744918412E+07
6	9.082863137099103E+07	9.08286313721744E+07	9.08286309363637E+07	9.082866346433716E+07
7	9.078051072980671E+07	9.07805107310266E+07	9.07805102219509E+07	9.078044788417752E+07
8	9.073603324690638E+07	9.07360332481548E+07	9.07360335549125E+07	9.073590592075115E+07
9	9.069499787832702E+07	9.06949978795886E+07	9.06949973086979E+07	9.069485134268293E+07
10	9.065715647138896E+07	9.06571564726498E+07	9.06571558871358E+07	9.065697424858394E+07
11	9.062226487996621E+07	9.06222648812127E+07	9.06222649572467E+07	9.062199518197852E+07
12	9.059009424836574E+07	9.05900942495852E+07	9.05900942700639E+07	9.058978473235501E+07
13	9.056043265334429E+07	9.05604326545285E+07	9.05604326277360E+07	9.056006897271423E+07
14	9.053308447634925E+07	9.05330844774908E+07	9.05330844107425E+07	9.053267170811471E+07
15	9.050786930120800E+07	9.05078693023010E+07	9.05078692020305E+07	9.050740733882987E+07
16	9.048462076982500E+07	9.04846207708656E+07	9.04846206427624E+07	9.048411291547363E+07
17	9.046318549584856E+07	9.04631854968308E+07	9.04631853458920E+07	9.046263105048560E+07
18	9.044342205541964E+07	9.04434220563413E+07	9.04434218869548E+07	9.044282086770603E+07
19	9.042520005476782E+07	9.04252000556290E+07	9.04252002214656E+07	9.042455537578163E+07
20	9.040839927007272E+07	9.04083992708709E+07	9.04083993981633E+07	9.040771641893551E+07
	RMSE	2.828798043478310E-03	1.29411362409527E+00	

Table 5(b): Approximate solutions of $N(t)$ for Model B

t	Exact Solutions	Approximate Solutions		
		$\rho-$SDIBBDF(2)	BBDF	ode15s
0	1.505249755000000E+08	1.50524975500000E+08	1.50524975500000E+08	1.505249755000000E+08
1	1.504513570960496E+08	1.50451357048880E+08	1.50451359518561E+08	1.504512353430396E+08
2	1.503463527588060E+08	1.50346352711325E+08	1.50346356990039E+08	1.503464165579907E+08
3	1.502404627785260E+08	1.50240462731177E+08	1.50240462349493E+08	1.502405238005271E+08
4	1.501406132664841E+08	1.50140613219326E+08	1.50140612636316E+08	1.501406670615670E+08
5	1.500480092156077E+08	1.50048009168616E+08	1.50048008462045E+08	1.500480409144854E+08
6	1.499624952252817E+08	1.49962495178423E+08	1.49962494386645E+08	1.499624755184070E+08
7	1.498836184571019E+08	1.49883618410340E+08	1.49883617555943E+08	1.498835260334835E+08
8	1.498108857239647E+08	1.49810885677263E+08	1.49810886172824E+08	1.498107141623161E+08
9	1.497438238086560E+08	1.49743823761984E+08	1.49743822827625E+08	1.497435980729780E+08
10	1.496819918811914E+08	1.49681991834527E+08	1.49681990877549E+08	1.496816975817238E+08
11	1.496249823887743E+08	1.49624982342095E+08	1.49624982466346E+08	1.496245407545826E+08
12	1.495724192953530E+08	1.49572419248638E+08	1.49572419282228E+08	1.495719132954510E+08
13	1.495239558275909E+08	1.49523955780823E+08	1.49523955737204E+08	1.495233615118667E+08
14	1.494792722424266E+08	1.49479272195597E+08	1.49479272086683E+08	1.494785978967502E+08
15	1.494380737310558E+08	1.49438073684153E+08	1.49438073520474E+08	1.494373191245911E+08
16	1.494000884771774E+08	1.49400088430194E+08	1.49400088221050E+08	1.493992589837297E+08
17	1.493650658644329E+08	1.49365065817359E+08	1.49365065570904E+08	1.493641600944542E+08
18	1.493327748231054E+08	1.49332774775938E+08	1.49332774499321E+08	1.493317926019450E+08
19	1.493030023056331E+08	1.49303002258371E+08	1.49303002529471E+08	1.493019490328421E+08
20	1.492755518809898E+08	1.49275551833629E+08	1.49275552041758E+08	1.492744362928245E+08
	RMSE	4.58492577404256E-02	1.17560581448876E+00	

Table 5(c): Numerical results for Model B

h	Method	TS	MAXE	TIME
10^{-2}	$\rho-$SDIBBDF(2)	1000	2.91834E-02	7.66111E-05
	BBDF	1000	1.00044E-01	1.46580E-04
10^{-4}	$\rho-$SDIBBDF(2)	100000	4.74320E-03	6.31006E-04
	BBDF	100000	1.03478E-02	7.96504E-03
10^{-6}	$\rho-$SDIBBDF(2)	10000000	5.89962E-04	6.39139E-02
	BBDF	10000000	1.03892E-03	4.03335E-01

Table 6(a): Numerical Approximation and Percentage Error for $C(t)$ in Model B

Time	$t = 5$		$t = 10$		$t = 15$		$t = 20$	
Method	Value	Error (%)	Value	Error (%)	Value	Error (%)	Value	Error (%)
True Value	9.088013651E+07	-	9.065702459E+07	-	9.050778143E+07	-	9.040834072E+07	-
$\rho-$SDIBBDF(2)	9.088032396E+07	0.00020626	9.065714920E+07	0.00013745	9.050786446E+07	0.00009173	9.040839604E+07	0.00006118
ode15s	9.088045744E+07	0.00035314	9.065697424E+07	0.00005553	9.050740733E+07	0.00041333	9.040771641E+07	0.00069054
Explicit Euler	9.088091461E+07	0.00085618	9.064156700E+07	0.01705062	9.049259639E+07	0.01677760	9.039496497E+07	0.01479481
Implicit Euler	9.087917647E+07	0.00105638	9.067108635E+07	0.01551094	9.052209811E+07	0.01581817	9.042116205E+07	0.01418157
Heun's	9.081316025E+07	0.07369735	9.065283625E+07	0.00461998	9.050789351E+07	0.00012383	9.040869663E+07	0.00039366
AM(4)	9.098329197E+07	0.11350715	9.065971329E+07	0.00296579	9.036363694E+07	0.15926198	9.025948965E+07	0.16464307
RK(4)	9.087922941E+07	0.00099813	9.065702233E+07	0.00000249	9.050778157E+07	0.00000015	9.040834085E+07	0.00000014

Table 6(b): Numerical Approximation and Percentage Error for $N(t)$ in Model B

Time	$t = 5$		$t = 10$		$t = 15$		$t = 20$	
Method	Value	Error (%)	Value	Error (%)	Value	Error (%)	Value	Error (%)
True Value	1.500476857E+08	-	1.496817763E+08	-	1.494379301E+08	-	1.492754561E+08	-
$\rho-$SDIBBDF(2)	1.500479913E+08	0.000203668	1.496819799E+08	0.000136021	1.494380657E+08	0.000090740	1.492755465E+08	0.000060559
ode15s	1.500480409E+08	0.000236724	1.496816975E+08	0.000052645	1.494373191E+08	0.000408865	1.492744362E+08	0.000683233
Explicit Euler	1.500296210E+08	0.012039305	1.496567244E+08	0.016736773	1.494131172E+08	0.016604151	1.492536018E+08	0.014640250
Implicit Euler	1.500641461E+08	0.010970112	1.497049896E+08	0.015508434	1.494613247E+08	0.015655061	1.492964046E+08	0.014033452
Heun's	1.500433604E+08	0.002882616	1.496821376E+08	0.000241378	1.494386008E+08	0.000448815	1.492760706E+08	0.000411655
AM(4)	1.500551132E+08	0.004950093	1.496819693E+08	0.000128940	1.494275502E+08	0.006945960	1.492647374E+08	0.007180483
RK(4)	1.500476206E+08	0.000043386	1.496817764E+08	0.000000066	1.494379303E+08	0.000000134	1.492754563E+08	0.000000134

Table 7(a): Approximate solutions of $S(t)$ for Model C

t	Approximate Solutions		
	$\rho-$SDIBBDF(2)	BBDF	ode15s
0	1	1	1
1	7.121767921953591E-01	7.121597468323849E-01	7.122242702847833E-01
2	5.105721108999255E-01	5.105482229232909E-01	5.106057882110795E-01
3	3.693253050261849E-01	3.693001996531895E-01	3.693468927136058E-01
4	2.703659949478694E-01	2.703425424177362E-01	2.703792104013361E-01
5	2.010338426872325E-01	2.010133036870709E-01	2.010408677791065E-01
6	1.524588543077552E-01	1.524415864773691E-01	1.524620198158161E-01
7	1.184265991543863E-01	1.184124848184946E-01	1.184263969786602E-01
8	9.458316800881166E-02	9.457186673388074E-02	9.458130796287531E-02
9	7.787815665318948E-02	7.786924918158092E-02	7.787550428748932E-02
10	6.617441306496098E-02	6.616747902998245E-02	6.617000205306466E-02

Table 7(b): Approximate solutions of $A(t)$ for Model C

t	Approximate Solutions		
	$\rho-$SDIBBDF(2)	BBDF	ode15s
0	0	0	0
1	9.142678545876823E-02	9.143905980819803E-02	9.141732921907264E-02
2	1.188714942531171E-01	1.188826206697272E-01	1.188696056981067E-01
3	1.171365258007368E-01	1.171430837032095E-01	1.171449159103748E-01
4	1.037575335900248E-01	1.037597611759942E-01	1.037688236631729E-01
5	8.722620550009369E-02	8.722534871691107E-02	8.723810549466401E-02
6	7.136731771310680E-02	7.136463018781980E-02	7.137712541637568E-02
7	5.765983469145690E-02	5.765627812729952E-02	5.766851344563632E-02
8	4.645402052917713E-02	4.645023748869594E-02	4.646026718248465E-02
9	3.759858741252527E-02	3.759496210502344E-02	3.760280629526270E-02
10	3.075494347049292E-02	3.075167685023055E-02	3.075823293020481E-02

The numerical results presented in Tables 4(a), 4(b), 5(a) and 5(b) compare the performance of the $\rho-$SDIBBDF(2) with the analytical solutions across two diabetes models i.e. Model A and Model B. For the two models, the approximate solutions generated by $\rho-$SDIBBDF(2) align closely with those from ode15s. The small difference observed are within acceptable error margins, demonstrating the effectiveness of $\rho-$SDIBBDF(2) in approximating solutions to ODEs. The $\rho-$SDIBBDF(2) method consistently shows results comparable to ode15s, affirming its stability and accuracy. Meanwhile, in a case where no theoretical solutions are provided for Model C, the solutions approximated by our method very much agree with the generated solutions by stiff MATLAB solver; ode15s as listed in Tables 7(a)– 7(e) and illustrated in Figures 10.

The numerical results reported in Tables 4(a), 4(b), 5(a) and 5(b) demonstrate the accuracy and robustness of the proposed $\rho-$SDIBBDF(2) method when applied to stiff diabetes models. For Model A, the proposed method yields RMSE values of 5.02E–03 for $C(t)$ and 8.59E–04 for $N(t)$ relative to the analytical solution, whereas the conventional BBDF method produces substantially larger errors of 5.41 and 2.33, respectively. Likewise, for Model B, the proposed method achieves RMSE values of 2.83E–03 for $C(t)$ and 4.58E–02 for $N(t)$, while the BBDF method yields errors exceeding unity for both state variables. These consistently low RMSE values indicate strong agreement with the analytical solutions and confirm the high accuracy of the proposed scheme.

Table 7(c): Approximate solutions of $T(t)$ for Model C

t	Approximate Solutions		
	$\rho-$SDIBBDF(2)	BBDF	ode15s
0	0	0	0
1	2.988925855072468E-02	2.988359125523819E-02	2.987828037672068E-02
2	9.036167950174147E-02	9.036009297503705E-02	9.034859758869425E-02
3	1.559418613379369E-01	1.559456967869050E-01	1.559233167505767E-01
4	2.156912178588185E-01	2.156990930240806E-01	2.156731606588106E-01
5	2.658572156996202E-01	2.658672975161552E-01	2.658411111913312E-01
6	3.060490926104724E-01	3.060598728844240E-01	3.060368019719632E-01
7	3.372901955904077E-01	3.373006534564913E-01	3.372805335469297E-01
8	3.610597589226197E-01	3.610693026986682E-01	3.610534286276254E-01
9	3.788489304955808E-01	3.788572835480100E-01	3.788451894249711E-01
10	3.919780991018668E-01	3.919851917903968E-01	3.919761518855799E-01

Table 7(d): Approximate solutions of $L(t)$ for Model C

t	Approximate Solutions		
	$\rho-$SDIBBDF(2)	BBDF	ode15s
0	0	0	0
1	1.406714671471442E-01	1.406876877630412E-01	1.406542668902658E-01
2	1.982545004722740E-01	1.982722925976809E-01	1.982484594468271E-01
3	2.101397823877811E-01	2.101533308413444E-01	2.101450726401809E-01
4	1.986875068126539E-01	1.986953903033596E-01	1.986983150765456E-01
5	1.769167172193587E-01	1.769194746142105E-01	1.769304797773686E-01
6	1.521091201448342E-01	1.521079798713679E-01	1.521226806009724E-01
7	1.280877936243780E-01	1.280840572103001E-01	1.281014722995577E-01
8	1.066425843117203E-01	1.066373650251528E-01	1.066543008345553E-01
9	8.840984264532223E-02	8.840398715949283E-02	8.841922548614718E-02
10	7.340612615570510E-02	7.340022289301923E-02	7.341480143605769E-02

The marked improvement over the standard BBDF approach shows that the proposed method is able to resolve both fast transient dynamics and slower disease–related responses more effectively in the coupled systems. As stiffness increases due to parameter variations governing metabolic response and disease progression, conventional solvers typically require smaller step sizes or tighter tolerances to preserve stability. In contrast, the proposed method maintains stable and accurate solutions across all tested regimes, highlighting its effectiveness in handling the coexistence of fast metabolic processes and slow pathological dynamics. In addition, the observed reduction in function evaluations confirms the computational efficiency gained from the singly diagonally implicit block structure.

The results in Tables 4(c) and 5(c) further confirm the accuracy and efficiency of the proposed $\rho-$SDIBBDF(2) method. For both Model A and Model B, reducing the step size h leads to a consistent decrease in the maximum error, in agreement with the RMSE trends reported earlier. Across all tested step sizes, the proposed method yields smaller maximum errors than the BBDF method, indicating improved local error control for stiff dynamics. Although both methods use the same number of steps, the proposed method requires significantly less execution time, particularly for finer step sizes. These results reinforce that the singly diagonally implicit block structure enables an efficient balance between accuracy and computational cost for stiff diabetes models.

Tables 6(a) and 6(b) present the results obtained from five numerical methods in [5], including ode15s, compared against the true values. By calculating the errors for $\rho-$SDIBBDF(2) and

Table 7(e): Approximate solutions of $P(t)$ for Model C

t	Approximate Solutions		
	$\rho-$SDIBBDF(2)	BBDF	ode15s
0	0	0	0
1	2.369674134450154E-02	2.369138200167566E-02	2.368768583054473E-02
2	7.539483372977143E-02	7.539155726101222E-02	7.538313008940964E-02
3	1.360078531771421E-01	1.360088243657533E-01	1.359925013203424E-01
4	1.954277535836592E-01	1.954327519627004E-01	1.954118749401809E-01
5	2.488413889041969E-01	2.488493206642614E-01	2.488260886229285E-01
6	2.944534086415827E-01	2.944630415767734E-01	2.944402251891216E-01
7	3.321018916002407E-01	3.321121691004696E-01	3.320902987894054E-01
8	3.624350941413294E-01	3.624452326201085E-01	3.624260233048476E-01
9	3.864365977024629E-01	3.864460815940736E-01	3.864299288909396E-01
10	4.051568916870104E-01	4.051719999137509E-01	4.051582865370054E-01

the other comparison methods, the accuracy of the proposed method can be evaluated. These tables summarize the computed values of $C(t)$ and $N(t)$ over a five–year period using the methods: $\rho-$SDIBBDF(2), ode15s, Explicit Euler, Implicit Euler, Heun's method, AM(4) and RK(4). Following AlShurbaji et al. [5], the years $5, 10, 15$ and 20 were selected for analysis, as significant changes were observed primarily at these intervals. The results clearly indicate that the $\rho-$SDIBBDF(2) method achieves high efficiency with minimal error percentages compared to the other numerical methods, with the exception of RK(4). Despite being a lower–order method, $\rho-$SDIBBDF(2) demonstrated performance comparable to that of higher–order methods, including RK(4).

The $L-$stable nature of the proposed method explains its robust performance for highly stiff regimes, where fast transient components are strongly damped. In contrast, ode15s requires significantly tighter tolerance settings to maintain convergence under the same conditions, leading to increased computational cost.

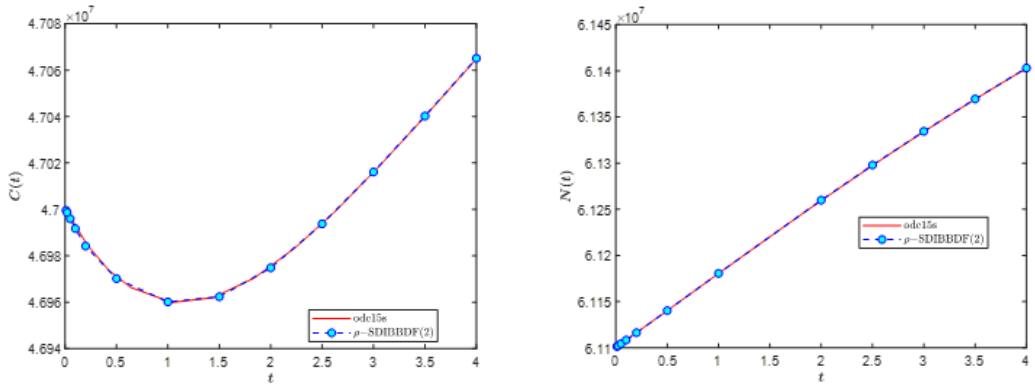

(a) Graph profiles for $C(t)$ (b) Graph profiles for $N(t)$

Figure 8: Solution curves of $\rho-$SDIBBDF(2) for Model A

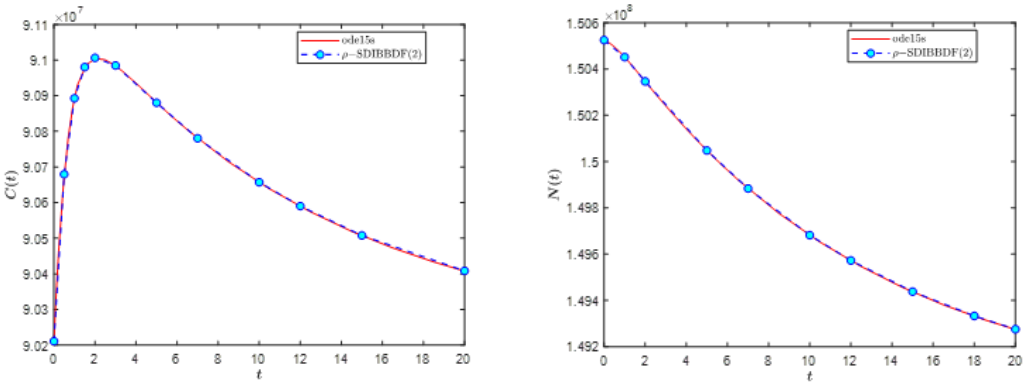

(a) Graph profiles for $C(t)$ (b) Graph profiles for $N(t)$

Figure 9: Solution curves of $\rho-$SDIBBDF(2) for Model B

Figures 8, 9 and 10 illustrate the temporal evolution of key state variables in the considered diabetes models under varying parameter settings. The smooth and non–oscillatory solution profiles produced by the proposed method reflect its strong stability properties, which are essential for accurately resolving stiff dynamics. Variations in model parameters governing insulin sensitivity, glucose uptake and complication progression directly influence the rate at which the system approaches equilibrium. Faster transient responses correspond to rapid metabolic processes, whereas slower trends represent long–term disease progression. These behaviours are consistent with physiological expectations and confirm that the numerical solutions preserve the underlying physical structure of the models. The ability of the proposed method to capture both short–term metabolic changes and long–term pathological effects without numerical instability further validates its suitability for realistic diabetes simulations.

Moreover, the results reveal that $\rho-$SDIBBDF(2) method effectively handles stiff equations, as evident in the close correlation of solution curves shown in Figures 8, 9 and 10. This correlation highlights the proposed method's capability in solving real–world dynamic systems modelled by ODEs efficiently.

In real–world applications, diabetes models are used to analyze disease progression, evaluate intervention strategies and support public health decision–making. Accurate numerical simulation is critical, as long–term predictions are sensitive to numerical instability and accumulated error. The proposed $\rho-$SDIBBDF(2) method provides a reliable computational tool for simulating such models over extended time horizons, making it suitable for studying intervention effects, complication risks and policy–level scenarios.

Overall, the combined numerical and physical analysis demonstrates that the proposed method not only achieves high numerical accuracy and efficiency but also preserves the qualitative behavior of diabetes models, thereby providing meaningful insights into real–world disease dynamics.

It should be noted that the present study is purely model–based and does not use clinical or population–level datasets. Consequently, issues related to population representativeness and potential biases in prescribing patterns do not directly affect the numerical results reported in this work. Such issues become relevant when diabetes models are calibrated or personalized using real clinical data. In future work, when applying the proposed numerical method to data–driven or personalized diabetes modelling, appropriate strategies such as stratified data selection, parameter calibration across diverse cohorts and sensitivity analysis will be required to mitigate potential

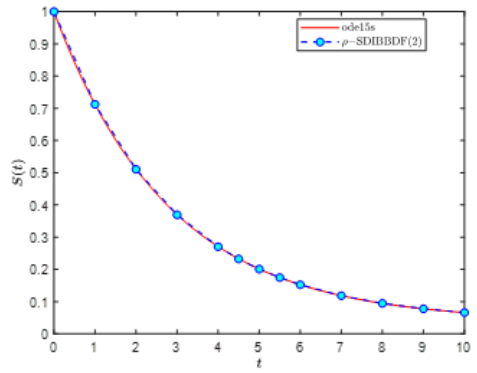

(a) Graph for $S(t)$

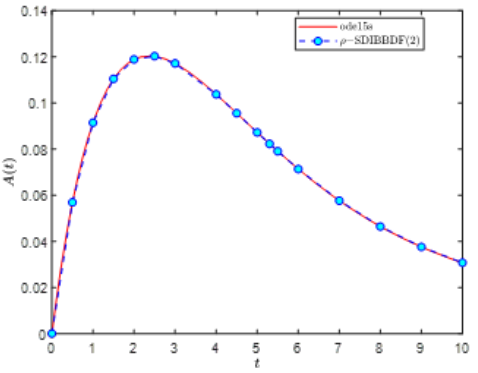

(b) Graph for $A(t)$

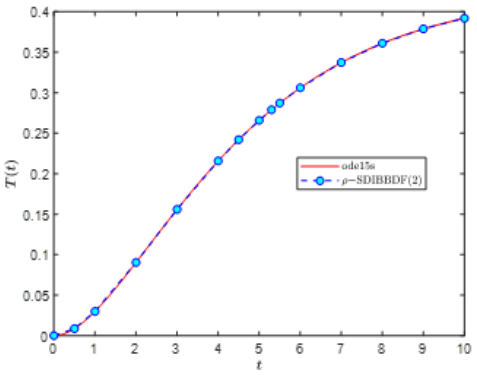

(c) Graph for $T(t)$

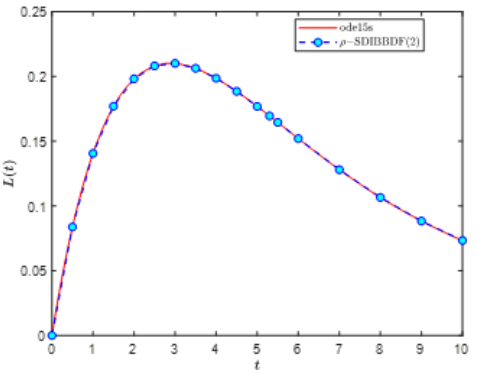

(d) Graph for $L(t)$

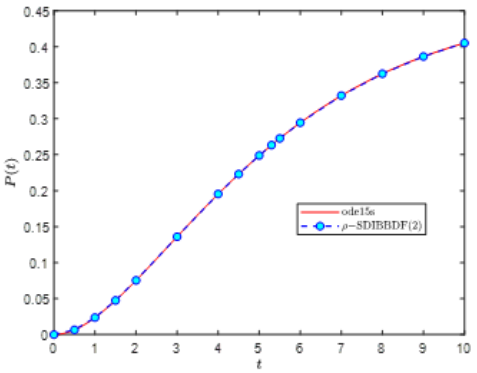

(e) Graph for $P(t)$

Figure 10: Solution curves of $\rho-$SDIBBDF(2) for Model C

biases and to ensure reliable and general predictions.

6 Conclusion

In conclusion, this research successfully employed the $\rho-$SDIBBDF(2) method to analyze the dynamics of diabetes mellitus. By leveraging advanced numerical techniques, the study examined the progression of diabetes, its complications and the impact of lifestyle interventions within various mathematical frameworks. The $\rho-$SDIBBDF(2) method demonstrated strong potential for efficiently solving ODE models. The approximate solutions generated were highly accurate and closely aligned with those produced by MATLAB's ode15s solver, confirming both the accuracy and stability of the proposed method in addressing complex, real–world systems.

From a physical perspective, the ability of the proposed $\rho-$SDIBBDF(2) method to maintain stability and accuracy over long time intervals is essential for modelling diabetes progression, where slow cumulative effects coexist with rapid metabolic changes. The numerical results demonstrate that the method can reliably capture these multiscale dynamics without artificial oscillations or loss of accuracy, supporting its applicability to realistic disease modelling and long–term simulation studies.

Despite the promising numerical performance demonstrated in this study, calibrating diabetes models of this complexity using real–world data remains a significant challenge. Key issues include parameter identifiability, inter-patient variability, limited availability of long–term clinical data and noise in measurement processes. Future research may address these challenges by incorporating systematic parameter estimation techniques such as nonlinear least squares optimization or Bayesian inference frameworks. In addition, coupling the proposed numerical method with sensitivity analysis and optimization-based calibration strategies may further enhance model reliability and predictive capability when applied to real clinical datasets.

Although the present study focuses on adult diabetes models and does not explicitly incorporate pediatric data or comorbid disease conditions, the proposed numerical framework remains broadly applicable. The models considered are parameter–based, and their structure allows adaptation to different population groups through appropriate parameter recalibration rather than fundamental model redesign. Moreover, the numerical method developed in this work is model–independent and can be readily extended to pediatric diabetes models or systems involving additional diseases when suitable data and formulations become available. As such, the absence of pediatric–specific data does not limit the general applicability of the proposed approach but instead highlights a natural direction for future extensions.

Overall, this study contributes valuable insights to the growing field of computational health sciences by strengthening the connection between mathematical modelling and practical diabetes–related health challenges and it provides a solid foundation for future research aimed at improving disease management strategies.

Acknowledgement This work was supported in part by the Ministry of Higher Education Malaysia through the Fundamental Research Grant Scheme Early Career Researcher 2024 (FRGS–EC/1/2024 /STG06/UITM/02/27). The authors also gratefully acknowledge the Center of Mathematical Sciences, Faculty of Computer and Mathematical Science, UiTM for supporting this research.

Conflicts of Interest The authors declare no conflict of interest.

References

[1] O. A. Akinfenwa, S. N. Jator & N. M. Yao (2013). Continuous block backward differentiation formula for solving stiff ordinary differential equations. *Computers and Mathematics with Applications*, *65*(7), 996–1005. https://doi.org/10.1016/j.camwa.2012.03.111.

[2] V. O. Akinsola & T. O. Oluyo (2019). Mathematical analysis with numerical solutions of the mathematical model for the complications and control of diabetes mellitus. *Journal of Statistics and Management Systems*, *22*(5), 845–869. https://doi.org/10.1080/09720510.2018.1556409.

[3] S. J. Aksah, Z. B. Ibrahim & I. S. M. Zawawi (2019). Stability analysis of singly diagonally implicit block backward differentiation formulas for stiff ordinary differential equations. *Mathematics*, *7*(2), 211. https://doi.org/10.3390/math7020211.

[4] A.-B. A. Al-Hussein & F. R. Tahir (2020). A new model for endocrine glucose-insulin regulatory system. *Iraqi Journal for Electrical and Electronic Engineering*, *16*(1), 1–8. https://doi.org/10.37917/ijeee.16.1.1.

[5] M. AlShurbaji, L. A. Kader, H. Hannan, M. Mortula & G. A. Husseini (2023). Comprehensive study of a diabetes mellitus mathematical model using numerical methods with stability and parametric analysis. *International Journal of Environmental Research and Public Health*, *20*(2), 939. https://doi:10.3390/ijerph20020939.

[6] M. S. Arif, K. Abodayeh & A. Ejaz (2023). On the stability of the diffusive and non-diffusive predator-prey system with consuming resources and disease in prey species. *Mathematical Biosciences and Engineering*, *20*(3), 5066–5093. https://doi.org/10.3934/mbe.2023235.

[7] M. S. Arif, K. Abodayeh & A. Ejaz (2023). Stability analysis of fractional-order predator-prey system with consuming food resource. *Axioms*, *12*(1), 64. https://doi.org/10.3390/axioms12010064.

[8] M. S. Arif, A. Ur Rehman & A. Ejaz (2025). Analysis of four-species diffusive and non-diffusive food chains using artificial neural networking. *European Scientific Journal*, *9*(2), 700–724. https://doi.org/10.28991/ESJ-2025-09-02-011.

[9] A. Boutayeb, E. H. Twizell, K. Achouayb & A. Chetouani (2004). A mathematical model for the burden of diabetes and its complications. *BioMedical Engineering OnLine*, *3*(20). https://doi.org/10.1186/1475-925X-3-20.

[10] J. C. Butcher (2008). *Numerical Methods for Ordinary Differential Equations*. John Wiley & Sons, England.

[11] I. Chervoneva, B. Freydin, B. Hipszer, T. V. Apanasovich & J. I. Joseph (2014). Estimation of nonlinear differential equation model for glucose-insulin dynamics in type I diabetic patients using generalized smoothing. *The Annals of Applied Statistics*, *8*(2), 886–904. https://doi.org/10.1214/13-aoas706.

[12] A. Ejaz, Y. Nawaz, M. S. Arif, D. S. Mashat & K. Abodayeh (2022). Stability analysis of predator-prey system with consuming resource and disease in predator species. *Computer Modelling in Engineering and Sciences*, *132*(2), 489–506. https://doi.org/10.32604/cmes.2022.019440.

[13] A. Ferdous (2023). An ordinary differential equation model for assessing the impact of lifestyle intervention on type 2 diabetes epidemic. *Healthcare Analytics*, *4*, Article ID: 100271. https://doi.org/10.1016/j.health.2023.100271.

[14] C. W. Gear (1971). *Numerical Initial Value Problems in Ordinary Differential Equations*. Prentice-Hall, New Jersey.

[15] J. Ha & A. Sherman (2020). Type 2 diabetes: one disease, many pathways. *American Journal of Physiology-Endocrinology and Metabolism*, *319*(2), 410–426. https://doi.org/10.1152/ajpendo.00512.2019.

[16] G. Hall & J. M. Watt (1976). *Modern Numerical Methods for Ordinary Differential Equations*. Oxford University Press, Oxford.

[17] Z. B. Ibrahim, N. Mohd Noor & K. I. Othman (2019). Fixed coefficient $A(\alpha)$ stable block backward differentiation formulas for stiff ordinary differential equations. *Symmetry*, *11*(7), 846. https://doi.org/10.3390/sym11070846.

[18] Z. B. Ibrahim, K. I. Othman & M. B. Suleiman (2007). Implicit $r-$point block backward differentiation formula for solving first-order stiff ODEs. *Applied Mathematics and Computation*, *186*(1), 558–565. https://doi.org/10.1016/j.amc.2006.07.116.

[19] H. M. Ijam & Z. B. Ibrahim (2019). Diagonally implicit block backward differentiation formula with optimal stability properties for stiff ordinary differential equations. *Symmetry*, *11*(11), 1342. https://doi.org/10.3390/sym11111342.

[20] C. A. Kennedy & M. H. Carpenter (2019). Diagonally implicit Runge-Kutta methods for stiff ODEs. *Applied Numerical Mathematics*, *146*, 221–244. https://doi.org/10.1016/j.apnum.2019.07.008.

[21] J. D. Lambert (1973). *Computational Methods in Ordinary Differential Equations*. John Wiley & Sons, New York.

[22] M. Y. Liu, L. Zhang & C. F. Zhang (2019). Study on banded implicit Runge-Kutta methods for solving stiff differential equations. *Mathematical Problems in Engineering*, *2019*(1). https://doi.org/10.1155/2019/4850872.

[23] A. Mari, A. Tura, E. Grespan & R. Bizzotto (2020). Mathematical modeling for the physiological and clinical investigation of glucose homeostasis and diabetes. *Frontiers in Physiology*, *11*, Article ID: 575789. https://doi.org/10.3389/fphys.2020.575789.

[24] A. C. Miller, N. J. Foti & E. Fox (2020). Learning insulin-glucose dynamics in the wild. *Proceedings of the 5th Machine Learning for Healthcare Conference*, *126*, 172–197.

[25] E. Ng, J. M. Kaufman, L. v. Veen & Y. Fossat (2022). A parsimonious model of blood glucose homeostasis. *PLOS Digit Health*, *1*(7). https://doi.org/10.1371/journal.pdig.0000072.

[26] N. M. Noor, S. A. M. Yatim & Z. B. Ibrahim (2024). Fractional block method for the solution of fractional order differential equations. *Malaysian Journal of Mathematical Sciences*, *18*(1), 185–208. https://doi.org/10.47836/mjms.18.1.11.

[27] S. P. Nørsett. Semi-explicit Runge-Kutta methods. Technical Report Reprint No. 6/74 Department of Mathematics, University of Trondheim Trondheim, Norway 1974.

[28] S. Qureshi, H. Ramos, A. Soomro, O. A. Akinfenwa & M. A. Akanbi (2024). Numerical integration of stiff problems using a new time-efficient hybrid block solver based on collocation and interpolation techniques. *Mathematics and Computers in Simulation*, *220*, 237–252. https://doi.org/10.1016/j.matcom.2024.01.001.

[29] W. E. Schiesser (2014). *Diabetes Glucose Tolerance Test*. John Wiley & Sons, Hoboken, New Jersey.

[30] G. M. Steil & J. Reifman (2009). Mathematical modeling research to support the development of automated insulin-delivery systems. *Journal of Diabetes Science and Technology*, *3*(2), 388. https://doi.org/10.1177/193229680900300223.

[31] M. B. Suleiman, H. Musa & F. Ismail (2015). An implicit $2-$point block extended backward differentiation formula for integration of stiff initial value problems. *Malaysian Journal of Mathematical Sciences*, *9*(1), 33–51. http://psasir.upm.edu.my/38950/.

[32] M. B. Suleiman, H. Musa, F. Ismail & N. Senu (2013). A new variable step size block backward differentiation formula for solving stiff initial value problems. *International Journal of Computer Mathematics*, *90*(11), 2391–2408. http://doi.org/10.1080/00207160.2013.776677.